J Soils Sediments (2011) 11:491–503
DOI 10.1007/s11368-010-0331-2

SOILS, SEC 3 • REMEDIATION AND MANAGEMENT OF CONTAMINATED OR DEGRADED SOILS • RESEARCH ARTICLE

Transport and re-entrainment of soil colloids in saturated packed column: effects of pH and ionic strength

Dongmei Zhou · Dengjun Wang · Long Cang · Xiuzhen Hao · Lingyang Chu

Received: 14 July 2010 / Accepted: 17 December 2010 / Published online: 14 January 2011

Abstract
Purpose Colloid migration in subsurface environments has attracted considerable attention in recent years because of its suspected role in facilitating transport of strongly adsorbed contaminants to groundwater. The influence of bulk solution pH or ionic strength on model colloid (i.e., latex microsphere, amorphous silica colloids) transport is well established, while little attention has been paid to water-dispersible soil colloids. In this study, saturated packed columns were conducted to explore the mechanism of transport and fate of water-dispersible soil colloids and facilitating transport of Cu during transients in solution chemistry.
Materials and methods Water-dispersible soil colloids were fractionated from a Cu-contaminated soil sample. Transport of soil colloidal suspensions was conducted with varying pH and ionic strengths, and then, re-entrainment of those retained colloids after completion the transport experiments was conducted by changing pore water solution transient ionic strength and pH conditions. Meanwhile, transport and fate of the Cu strongly adsorbed on the soil colloids were determined under different ionic strength conditions.
Results and discussion The transport behavior of soil colloids in porous media was found to depend on the pH and ionic strengths of bulk solution. An increase in solution ionic strength and decrease in solution pH resulted in greater deposition which was revealed by the collision efficiency (α). It increased from 0.15 to 1.0 when solution composition changed from 0 to 50 mM $NaNO_3$ and decreased dramatically from 1.0 to 0.035 as the solution pH converted from 2.97 to 8.94. The results were in agreement with Derjaguin–Landau–Verwey–Overbeek theory. Upon stepwise reduction in ionic strength of eluting fluid or enhancement in its pH, a sharp release of colloids retained in the column occurred in each step. Meanwhile, the value of FRE_{NaOH} that reveals the effect of NaOH solution at pH 11 on the mobilization of retained colloids deposited in the primary minimum increased from 38.6% to 64.6% when the ionic strength of bulk solution changed from 0 to 50 mM $NaNO_3$ and decreased from 86.7% to 35.8% as the solution pH from 2.97 to 8.94. In addition, the transport and fate of the Cu strongly adsorbed on soil colloids were highly consistent with the results of soil colloids.
Conclusions The colloid collision efficiency (α) decreased as the pH of bulk solution increased and increased as the ionic strength of bulk solution increased in saturated columns packed with pure quartz sand, and NaOH solution at pH 11 poses a predominant role on mobilization of the retained colloids deposited in the primary minimum. Meanwhile, the strongly adsorbed Cu on soil colloids almost cannot be detached from its carrier under the competition of coexisted cations in the bulk solution and cotransport with its carrier under different ionic strengths.

Responsible editor: Willie Peijnenburg

D. Zhou (✉) · D. Wang · L. Cang · X. Hao · L. Chu
State Key Laboratory of Soil and Sustainable Agriculture,
Institute of Soil Science, Chinese Academy of Sciences,
71st East Beijing Road,
Nanjing 210008, People's Republic of China
e-mail: dmzhou@issas.ac.cn

D. Wang
Graduate School of the Chinese Academy of Sciences,
Beijing 100049, People's Republic of China

L. Chu
College of Resources and Environmental Sciences, Anhui Agricultural University,
Hefei 230036, People's Republic of China

Keywords Cotransport · DLVO theory · Ionic strength (IS) · pH · Water-dispersible soil colloids (WDSC)

1 Introduction

Transport of soil colloids in subsurface environments is a potentially critical mechanism contributing to the movement of contaminants that absorbed to solids (McCarthy and McKay 2004). Another concern of soil colloid movement is the deposition of mobile soil colloids that may reduce soil permeability (Baveye et al. 1998). Colloids are generally considered to be particles with effective diameters of around 10 nm to 10 μm, with the smallest colloids just larger than dissolved macromolecules, and the largest colloids being those that resist settling once suspended in soil pore water (DeNovio et al. 2004). Soil colloids in natural subsurface environments include mineral precipitates (notably iron, aluminum, calcium, and manganese oxides, hydroxides, carbonates, silicates, and phosphates), rock and mineral fragments (including layer silicates, oxides, and other weathering products of mineral phases), microbes, and plant decay debris which contains a great abundance of particles in the colloidal size range (Posadas et al. 2001). While a theoretical framework exists for elaborating the transport of synthetic model colloids (i.e., latex microsphere (Bradford et al. 2002; Tufenkji and Elimelech 2005), amorphous silica colloids (Elimelech et al. 2000), and ceramic microspheres (Li et al. 2006) in model systems (i.e., quartz sand (Torkzaban et al. 2008), and glass beads (Bradford et al. 2002)), the principle issue that limits prediction is comprehending of how natural soil colloids behave in natural subsurface systems. However, natural systems, which are mainly composed of soils and sediments, have complex physicochemical properties such as different contents of clay, total organic carbon, and Fe (Ferreira et al. 2010), large variability in the shape, size, and roughness, and surface charge properties of minerals and sediments (Gerbersdorf et al. 2007; Jaisi and Elimelech 2009). So far, most of our studies have been paid on the transport behavior of synthetic model colloids in model or natural systems (Bradford et al. 2002; Elimelech et al. 2000; Jaisi and Elimelech 2009), while little research has been paid on the transport and fate of natural colloids. Therefore, in this experiment, water-dispersive soil colloids were used as model colloids, and quartz sand was selected as model system to systematically investigate the effects of solution chemistry (transient pH and ionic strengths (ISs)) on the transport and re-entrainment of the soil colloids in saturated packed column.

The influence of bulk solution pH or IS on colloid transport has been well established. The expected effect—increased deposition at lower pH or higher ISs—is attributed to decreasing of repulsive surface interaction energies between colloids and colloids, and colloids and grain surfaces (Grolimund et al. 1998). Switching the eluting fluid to lower IS or higher pH enhances colloid release due to increased electrostatic repulsion and a corresponding increase in the double layer thickness (Ryan and Elimelech 1996). In natural environment, aquifer matrices (e.g., quartz sand) and soil colloids possess a net negative surface charge at the prevailing pH conditions, thus leading to unfavorable attachment conditions (Wan and Tokunaga 2002). In this case, Derjaguin–Landau–Verwey–Overbeek (DLVO) theory (Derjaguin and Landau 1993; Verwey and Overbeek 1948) introduces the attractive primary minimum, the maximum repulsive energy barrier (Φ_{max}), the attractive secondary minimum (Φ_{min2}), or all (Ryan and Elimelech 1996). Recently, the research results of model colloids documented that the secondary minimum disappeared when transient solution IS converted to zero (Lenhart and Saiers 2003). Meanwhile, Tosco et al. (2009) demonstrated that the colloids deposited in primary minimum cannot be re-entrained into pore water solution through lowering IS of the eluting fluid, and a high pH solution (NaOH solution at pH 11) is able to force the mobilization of these retained colloids. However, no systematic investigation has been made to examine the extent of high pH solution in promoting the re-entrain of those retained colloids into pore water solution.

Interest in soil colloids behavior in porous media arose from the recognition that colloids might be crucial in facilitating transport of the contaminants strongly adsorbed on them. The contaminants may be cations (e.g., Cu^{2+}, Cs^{+}, Cd^{2+}), anions, and nonpolar and polar organic compounds, and the cationic forms of metals are the most frequently reported contaminants influenced by colloid-facilitated transport (Kersting et al. 1999; Sen et al. 2002) because those cationic forms of metals (such as Cu, Cd, and Zn) have a large tendency to sorb to soil colloids such as clay minerals, metal (hydro)oxides, and humic acid (Bradl 2004; Usman et al. 2005). In the experiment, the contaminant (Cu) adsorbed on the soil colloids might be cotransported with its carrier or detached from its vector under the competition of coexisted cations in the bulk solution during the whole transport experiment. Hence, it is significantly necessary to investigate the transport and fate of Cu in the presence of coexisted cations under different ISs of the bulk solution.

The objectives of this study were to systematically investigate the effects of (1) solution chemistry (transient pH and IS) on the transport and fate of soil colloids in saturated porous media under unfavorable attachment conditions, (2) NaOH solution at pH 11 on the mobilization of retained colloids deposited in the primary minimum, and (3) coexisted cations on the transport and fate of Cu under different ISs.

2 Experimental materials and procedures

2.1 Granular porous media

Quartz sand (Sinopharm Chemical Reagent Co., Ltd, China) with median grain size (d_{50}) of 500 μm was used as the packing material for column experiments. The uniformity index ($U_i=d_{60}/d_{10}$, where x% of the mass was finer than d_x) of the quartz sand was 1.20 as provided by the manufacturer. Prior to use, the sands were ultrasonicated in 0.01 M NaOH solution for 30 min, rinsed with deionized water, and then ultrasonicated again for an additional 30 min in 0.01 M HCl solution before a final thorough rinsing with deionized water. The sands were then dried in an oven at 105°C. Cleaned sands were stored in PTFE plastic bottles.

2.2 Soil colloids

Water-dispersible soil colloids (WDSC) were fractionated from a Cu-contaminated soil sample (CSS) located at Guixi, Jiangxi Province, China, following the procedures described by Xiong et al. (1985). A liter of deionized water was added to 0.1 kg of the soil particles (through 60-mesh nylon sieve), and the suspension was ultrasonicated for 30 min. Then, the mixture was stirred for 1 min to disperse the suspension. Afterward, the supernatant (particle sizes were less than 2 μm) was decanted at the fixed time according to Stokes Law. The above process was repeated several times to ensure that the electrical conductivity of the supernatant was smaller than 0.01 ds m^{-1}. Colloidal particles were separated from the extracted solution by gravity setting, air-dried, gently crushed, passed through a 100-mesh nylon sieve, and stored in a polyethylene bottle. Colloidal suspensions were prepared by redispersing the air-dried colloids in ultrapure water (18.2 MΩ, Millipore, Inc., USA) and sonication for 20 min. Physicochemical properties of the CSS and WDSC are shown in Table 1.

2.3 Packed-bed column

Colloid transport experiments were conducted in glass chromatography column packed with quartz sand. The column was 26 mm in diameter and 200 mm in length, and was fitted with an 80-μm wire mesh at both ends. Column characteristics were determined through fitting of conservative tracer (chloride) breakthrough curves. The porosity of the packed columns was determined gravimetrically, and it varied between 0.36 and 0.40. Each column was packed carefully following the same procedure to ensure reproducibility between the columns.

2.4 Experiment procedures

Analytical reagent-grade $NaNO_3$ and ultrapure water were used to prepare electrolyte solutions at different ISs. Solution pH for all the colloidal suspension solution was adjusted by 0.01 M HCl or 0.01 M NaOH. Column experiments were performed over a range of ISs (0, 1, 10, and 50 mM $NaNO_3$) and pH (2.97, 4.98, 7.00, and 8.94).

The packed column was initially equilibrated by flushing several pore volumes (PVs) of ultrapure water, and at least 5 PVs of the colloid-free background electrolyte solution at the specific ISs was employed for each deposition in order to establish a steady-state flow and to standardize the chemical conditions. Experiments were then performed in several phases (detailed experiment procedures are provided in Table 2): (1) initially, colloidal particles suspended in the same initial solution chemistry (0, 1, 10, and 50 mM of $NaNO_3$ for the experiments, respectively) were injected into the column by the peristaltic pump upward at the constant flow rate (0.95 cm min^{-1}) about several PVs, part of which were retained in the packed column; (2) secondly, several PVs of particle-free background electrolyte solution were pumped into the column to ensure that almost no colloid was detected in the effluent; (3) in the third phase, the

Table 1 Physicochemical properties of the CSS and the WDSC used in the experiments

	pH[a]	OM[b], g kg^{-1}	CEC[c], cmol kg^{-1}	TEB[d], cmol kg^{-1}	Total Fe[e], g kg^{-1}	Total Al[e], g kg^{-1}	Total Cu[e], mg kg^{-1}	Mean colloid diameter, μm
CSS	5.3	6.6	13.4	9.1	37.5	9.5	317	ND
WDSC	5.1	8.8	28.6	13.5	74.6	13.9	700	0.75[f]

ND not determined

[a] pH, pH electrode (soil:water=1:2.5)

[b] Organic matter, potassium dichromate–capacity act

[c] Cation exchange capacity

[d] Total exchangeable bases, 1 M ammonium acetate (pH 7.0)

[e] Total Fe, and Al, and Cu, HF:$HClO_4$:HNO_3=2:1:1

[f] Measured by TEM (JEM-2100, Japan)

Table 2 Detailed experiment procedures at different pH and ISs, and mass recovery from different phases, and the effect of NaOH solution (FRE_{NaOH})

Expt	pH	IS[a] mM	Approach velocity cm min^{-1}	Dispersion coefficient cm^2 min^{-1}	PV_0[b]	MR_{12} (%)[c]	MR_3 (%)[d]	MR_4 (%)[d]	MR_s (%)[e]	MR_{Total} (%)[f]	FRE_{NaOH} (%)[g]
1	2.97	0	0.96	0.12	6.0	0.7	86.1	ND	13.2	86.9	86.7
2	4.98	0	0.98	0.11	6.0	75.9	13.1	ND	11.0	89.0	54.4
3	7.00	0	0.97	0.11	6.0	80.4	9.9	ND	9.7	90.3	50.5
4	8.94	0	0.91	0.10	6.0	89.4	3.8	ND	6.8	93.2	35.8
5	5.00	0	0.96	0.10	3.5	84.4	3.7	4.6	7.3	92.7	38.6
6	5.00	1	0.97	0.11	3.5	79.9	7.4	4.5	8.2	91.8	35.4
7	5.00	10	0.92	0.12	3.5	48.8	34.0	8.1	9.2	90.8	46.8
8	5.00	50	0.96	0.10	3.5	1.7	68.5	19.2	10.7	89.3	64.6

ND not determined

[a] Here, IS of the bulk solution at different pH condition is approximately equal to zero

[b] PV_0, colloid pulse during phase 1 in terms of pore volumes

[c] MR_{12}, fraction of mass recovery of the injected colloids from phases 1 and 2

[d] MR_3 and MR_4, fraction of mass recovery of the injected colloids from phase 3 and phase 4, respectively

[e] MR_s, fraction of mass recovery of the injected colloids from dissection experiment

[f] MR_{Total}, fraction of mass recovery of the injected colloids during phases 1, 2, 3, and 4 for different ISs, and phases 1, 2, and 3 for different pH conditions

[g] Effect of NaOH solution at pH 11 as provided in Section 3

retained colloids were re-entrained by injecting ultrapure water (IS=0); (4) the last step of each experiment was flushing a pH 11 colloid-free solution (achieved by addition of NaOH) to force the mobilization of all unreleased particles; and (5) following completion of the colloid transport and re-entrainment experiments, the dissection experiment was conducted. Briefly, the end fitting was removed, and the saturated porous media were carefully excavated into glass centrifuge tubes. Excess eluant solution was added to fill the centrifuge tubes. These tubes were slowly shaken for several hours to liberate strained colloids, and the concentrations of the colloids in the excess aqueous solution (decanted from the tubes) were measured. Column outflow was collected into a 15-mL glass tube in regular time intervals using a fraction collector.

2.5 Analytical procedures

2.5.1 Characterization of the WDSC

Transmission electron microscopy (JEM-2100 TEM, Japan) was used to determine the diameter of soil colloids, and the sample was prepared by placing a droplet of the soil colloidal suspension (200 mg L^{-1}) on a Cu mesh TEM grid. Phase identification of the WDSC was carried out on X-ray diffraction (Shimadzu XRD-6000, Japan) with Cu-K_α radiation (wavelength, λ=0.15406 nm). The scanning range (2θ) was from 10° to 80° at a speed of 5° min^{-1}.

2.5.2 Electrokinetic potential of granular porous media

The particles from pulverized quartz sand (approximately 2 μm) were used as surrogates for the quartz surface and are further referred to as quartz particles for electrophoretic mobility measurement. To prepare quartz sand particles, we pulverized the quartz sand into small particles with an agate mortar. The small particles were suspended in solutions with corresponding ionic strengths and pH conditions as we conducted in the colloids transport experiment, and the solutions were sonicated for 1 h. Aliquots (5 mL) of the supernatant containing quartz particles were used for electrophoretic mobility measurement using a microelectrophoresis instrument (JS94G, Shanghai Zhongcheng Digital Technology Co., Ltd, China). The values of zeta potential (ζ-potential) were calculated using computer with the specific software based on the Helmholtz–Smoluchowski equation (Hunter 1981).

2.5.3 Electrokinetic potential of soil colloids

Triplicate soil colloid suspensions with a concentration of 200 mg L^{-1} at fixed pH or ionic strength were used for the microelectrophoresis instrument at 25°C.

2.5.4 Concentration of soil colloids and Cu in the effluent

Colloid concentrations in the outflow were determined by UV/Vis spectrophotometer (721–100, Shanghai Jinghua

Science and Technology Instrument Co., Ltd, China), at a wavelength of 420 nm (Goldberg and Forster 1990). A calibration curve was constructed by diluting of 200 mg L^{-1} colloid suspension. Colloid concentration in the range of 0–200 mg L^{-1} versus spectrometer response was linear with a coefficient of determination of R^2=0.999, and the lower detection limit is approximately equal to 1.0 mg L^{-1}.

Aliquots (5 mL) of all effluents were centrifuged at 9,000×g for 10 min, and then filtered through a 0.22-μm membrane filter to determine the dissolved Cu (0.22 μm as the operational cutoff for colloid-free Cu). Other aliquots (5 mL) of all effluents were added with 5 mL of 16 M HNO_3 to determine the total Cu. Particulate Cu (colloid-facilitated Cu) was calculated as the difference between dissolved and total Cu. The Cu concentration was determined by Atomic Absorption Spectrophotometer (Hitachi Z-2000 AAS, Japan).

The chloride tracer, which was used to determine the hydrodynamic performance of the column, was analyzed by chloride ion-selective electrode. Based on the tracer concentration data and measured pore water velocity (V), the dispersion coefficient (D) of the porous media was determined by fitting the standard convection–dispersion equation for a conservative solute to the chloride breakthrough curves using the CXTFIT 2.1 program. Colloid concentrations in the outflow were related to the concentrations in the inflow and represented as relative concentrations C_i/C_0.

3 Data analysis

The fraction of mass recovery (MR_{12}) of the injecting soil colloids during phases 1 and 2 was calculated by the zero moment by integrating a soil colloid breakthrough curve and normalizing it to the total injected amount:

$$MR_{12}(\%) = \frac{\int_0^{T_0} Q(t)C(t)dt}{\int_0^{T_0} Q(t)C_0(t)dt} \times 100\% \quad (1)$$

where Q is the flow rate (L^3 T^{-1}), C_0 and C are the concentrations of soil colloids in solution for the injection solution and column outflow, respectively (M L^{-3}), t is the time (T), and T_0 is the duration of the pulse (T). Here, T_0 is the duration time during phases 1 and 2.

The collision efficiency (α), which is defined as the probability of a collision between a particle and grain resulting in attachment of the particle (Harvey and Garabedian 1991), can be determined by:

$$\alpha = -\frac{2}{3}\frac{d_c 1n(MR_{12})}{(1-\varepsilon)L\eta_0} \quad (2)$$

where d_c is the diameter of quartz sand, ε is the porosity, L is the column length, and η_0 is the theoretical single collector contact efficiency calculated using the TE equation (Tufenkji and Elimelech 2004):

$$\eta_0 = 2.4A_s{}^{1/3}N_R^{-0.081}N_{Pe}^{-0.715}N_{vdW}^{0.052} + 0.55A_sN_R^{1.675}N_A^{0.125} + 0.22N_R^{-0.24}N_G^{1.11}N_{vdw}^{0.053} \quad (3)$$

where A_s is porosity-dependent parameter, N_R is the aspect ratio, N_{Pe} is the Peclet number, N_{vdW} is the van der Waals number, N_A is the attraction number, and N_G is the gravity number. All the mentioned parameters in the TE equation are listed in Table 3.

DLVO theory was used to calculate the total interaction energy (sum of London–van der Waals attraction and electrostatic double layer repulsion) for soil colloidal particles upon close to approach to quartz sand surfaces (assuming sphere–plate interactions) for different ISs (IS= 1, 10, and 50 mM). Retarded London–van der Waals attractive interaction force was determined from the expression of Gregory (1981) utilizing a value of 1.0×10^{-20} J for the Hamaker constant. In these calculations, constant potential electrostatic double layer interactions were quantified using the expression of Hogg et al. (1966), with ζ-potentials in place of surface potentials (Table 4).

The fraction of mass recovery of the retained colloids, FRE_{NaOH}, which was recovered during flushing NaOH solution at pH 11, was calculated as follows:

$$FRE_{NaOH}(\%) = \frac{\text{Mass recovery during injecting NaOH solution}}{\text{Mass of deposited colloids before injecting NaOH solution}} \times 100\% \quad (4)$$

In practice, FRE_{NaOH} represents the fraction of colloidal particles that were detached from the porous media during

Table 3 Parameters used in the calculation of the single collector contact efficiency (η_0) and collision efficiency (α) for WDSC

Parameters	
Collector diameter (μm)	500
Porosity (ε)	0.36–0.40
Diameter of soil colloids (μm)	0.75
Absolute temperature (K)	293
Darcian velocity (cm min^{-1})	0.91–0.98
Fluid density (g cm^{-3})	1.00
Fluid viscosity (N sm^{-2})	1.0×10^{-3}
Hamaker number (J)	1.0×10^{-20}
Column length (cm)	20
Gravity (m s^{-2})	9.81
Boltzmann constant (J k^{-1})	1.38×10^{-23}

Table 4 Electrokinetic properties of soil colloids and quartz sand as well as the calculated depth of the repulsive energy barrier (Φ_{max}), the attractive secondary minimum (Φ_{min2}), and the distance of the secondary minimum from the quartz sand surface (h)

Ionic strength, mM	ζ-Potentials (mV)		Φ_{max} (K_bT_K)	Φ_{min2} (K_bT_K)	h (nm)
	Quartz sand	Soil colloids			
0	−67	−73	ND	ND	ND
1	−60	−45	166	−1.1	73
10	−37	−32	74	−3.5	17
50	−21	−25	29	−6.8	6

ND not determined

flushing NaOH solution at pH 11 relative to those that were retained in the porous media before injecting the NaOH solution. It is generally accepted that the NaOH solution at high pH can promote the re-entrainment of those retained colloids deposited in the primary minimum; therefore, the above formula (Eq. 4) makes it possible to investigate the effect of NaOH solution on re-entrainment of colloids retained in the primary minimum.

4 Results and discussion

4.1 Characterization of the WDSC

TEM has often been used to visualize the shape and size of aquatic colloids (Wilkinson et al. 1999). The TEM images of WDSC (Fig. 1) show that most colloidal particles are irregular in shape (spheroidal, sheet, and hexagonal), and with board size distributions (mean diameter is about 0.75 μm). It is generally accepted that the relatively thick and regular (hexagonal) platy particles are kaolinites (see Fig. 1b) which are confirmed by XRD of the WDSC. That the reflection peaks at 2θ=34.897° and 38.199° are characteristic of kaolinites, and the reflection peaks at 2θ=19.846°, 26.668°, 61.799°, and 62.121° (Fig. 2) correspond to montmorillonites, which possess relatively small and sheet particles as revealed in Fig. 1a. The main physicochemical properties of the CSS and WDSC are reported in Table 1. Their pH and organic matter (OM) are similar. Notice that the concentration of OM of WDSC is up to 8.8 mg kg^{-1}, and the OM probably possesses a small portion of humic acid because soil OM refers to the organic compounds from decomposed plant/animal products with humic and fulvic acids as two of mainly fractions (Grafe et al. 2001). The other properties such as CEC, total Fe, Al, and TEB are slightly higher for WDSC than CSS which are

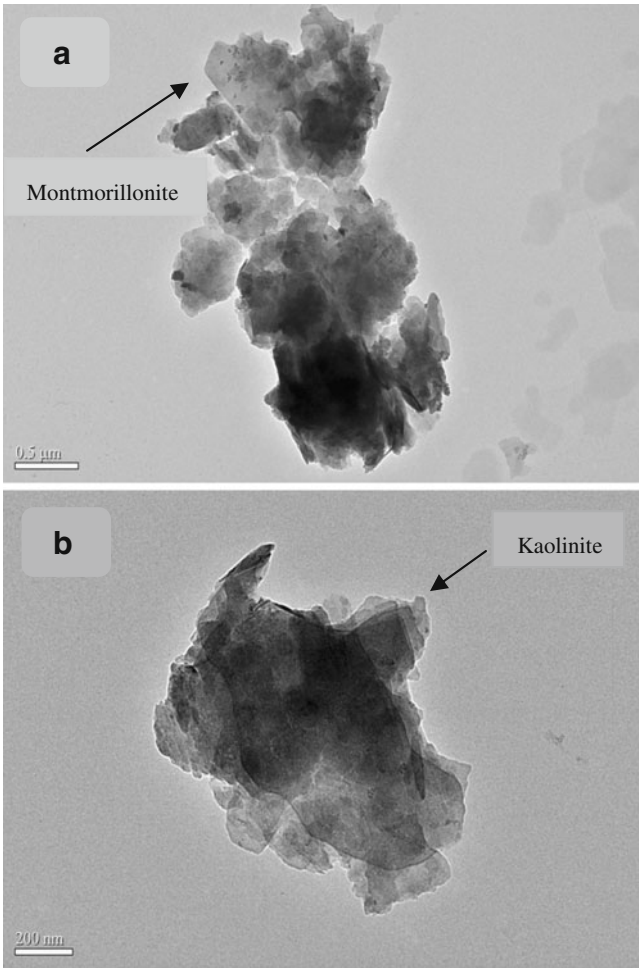

Fig. 1 TEM observation of the WDSC at two levels of magnification. **a** *Scale bar* 0.5 μm. **b** *Scale bar* 200 nm

in agreement with the results of Karathanasis (1999). Particularly, the Cu adsorbed on WDSC attains the concentration as high as 700 mg kg^{-1} which strongly affects the surface charge and ζ-potential of its vector. In

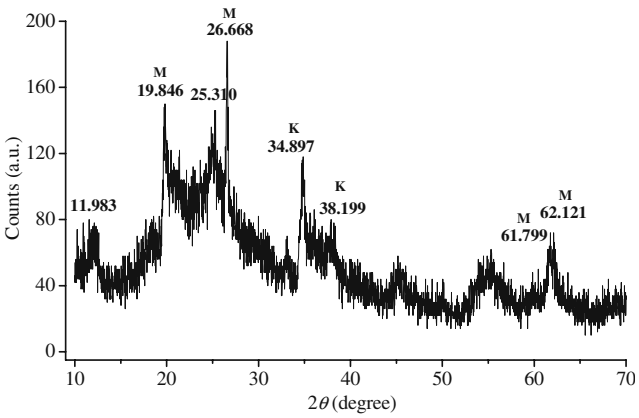

Fig. 2 XRD of the WDSC. Note that *K* and *M* denote the characteristic reflection peaks of kaolinite and montmorillonite, respectively

addition, Fe and Al (hydro)oxides that exist in WDSC possess positive surface charge at the prevailing pH conditions, making partly contribution to the ζ-potential of the WDSC.

4.2 Electrokinetic potentials (ζ) of soil colloids and quartz sand

Variations in the ζ-potentials as a function of solution pH and ionic strengths are shown in Fig. 3. Electrophoretic mobilities were converted to ζ-potentials using the well-known Helmholtz–Smoluchowski equation. As observed, both the soil colloids and quartz sand are negatively charged, and their ζ-potentials become less negative with decreasing pH and increasing IS of the bulk solution. Those ζ-potentials increased from −0.71 mV to −67 mV (more negative) of soil colloids and from −12 mV to −59 mV of quartz sand when solution pH increased from 2.97 to 8.94. As solution pH decreased, the surface charges of colloidal particles were neutralized by the H^+ ions of the bulk solution. Therefore, the net surface charge decreased which make the ζ-potentials less negative. Similar result has been observed by other researchers (Bradford et al. 2002; Kretzschmar et al. 1998). That the ζ-potentials decreased with increasing bulk ionic strengths can be explained by the compression of the electrostatic double layers and reduction of the Stern potential at high ionic strength (Hunter 1986).

4.3 Representative breakthrough curves of soil colloids at different solution pH and ISs

Deposition and re-entrainment experiments with varying chemical conditions, similar to those employed in the electrophoretic mobility measurements, were conducted. The results are presented in the form of representative breakthrough curves, i.e., the fraction of the influent particle concentration leaving the packed bed, C_i/C_0, as a function of PVs. Typical colloids breakthrough curves at different bulk solution pH conditions are presented in Fig. 4. As observed, when the pH was higher than or equal to 4.98, the effluent concentrations increased slowly with PV toward a steady-state level. However, more than 99% of the input soil colloids were retained in the packed column at the solution pH of 2.97 for the pH that was close to the pH_{PZC} of quartz sand (pH_{PZC} 2–3). The results can be explained by DLVO theory, that is, as solution pH increased, the ζ-potentials of soil colloids and quartz sand increased (more negative) which enhanced the electrostatic double layer repulsion interaction while the attractive London–van der Waals interaction was independent of the solution chemistry (Elimelech et al. 1995). The height of the Φ_{max} increased, and consequently, much more soil colloidal particles could migrate out of the packed bed.

The PV-dependent trend observed in the rising limb of the breakthrough curves indicated that either the retention sites were being filled up during the colloid injection which is called "blocking" in which the deposited colloids inhibited the attachment of approaching particles (Elimelech and Omelia 1990) or simultaneous detachment of the deposited colloids was occurring during the colloid transport experiment (Torkzaban et al. 2008). The latter seemed to be a more likely explanation because detachment produced insignificant tailing in the breakthrough curves as observed in the transport experiment (see Fig. 3a).

The breakthrough curves obtained from the experiments conducted with different ISs of bulk solution (Fig. 5) exhibited a similar trend under transient solution chemical conditions. However, some different or opposite results were observed when the initial bulk solution ionic strength was 10 mM. The PV-dependent trend observed in the falling limb of the breakthrough curves at the IS of 10 mM indicated that the aggregation of colloidal particles was quite more obvious during the transport experiment. Therefore, it was inferred that the "critical salt concentration" (Khilar and Fogler 1984) was below 10 mM $NaNO_3$ for the colloidal suspension used in the experiments.

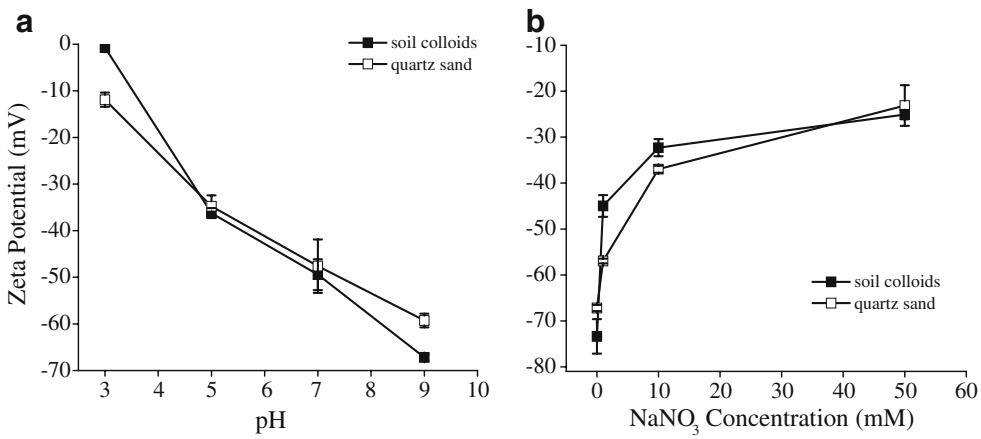

Fig. 3 ζ-Potentials of soil colloids and quartz sand under **a** different bulk solution pH conditions (0 mM $NaNO_3$ concentration) and **b** different bulk solution ionic strength conditions (pH=5.0)

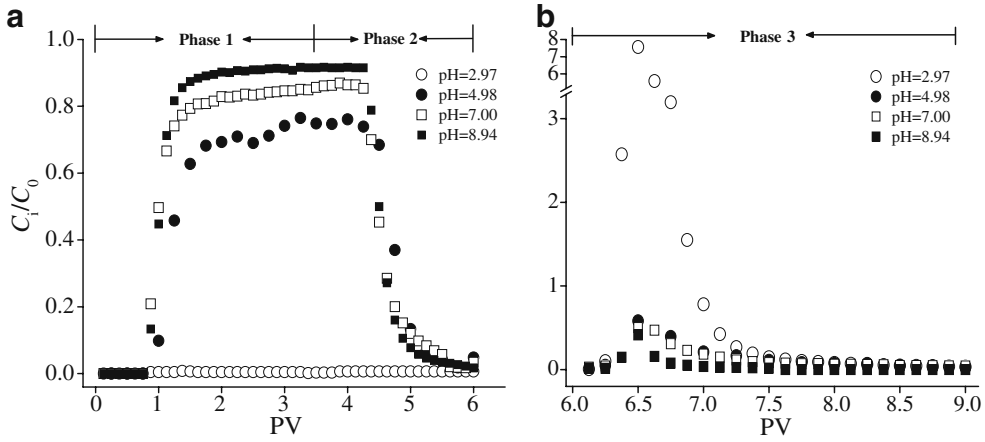

Fig. 4 Representative breakthrough curves for soil colloids at different bulk solution pH conditions. **a** Phase 1: 0–3.5 PVs, colloidal particles suspended in different pH solution; phase 2: 3.5–6.0 PVs, colloid-free background electrolyte solution. **b** Phase 3: 6.0–9.0 PVs, colloid-free NaOH solution at pH 11

Figure 6 and Table 4 present the calculated soil colloid–quartz sand interaction energy from DLVO theory when ISs of the bulk solutions were 1, 10, and 50 mM. Results indicate that colloid–sand interactions are repulsive, and that the height of Φ_{max} decreases and the depth of the Φ_{min2} increases, respectively. At ISs equal to or less than 50 mM, the DLVO calculations predict the presence of substantial repulsive energy barriers (ranging from 29 K_bT_K at 50 mM to 166 K_bT_K at 1 mM, where K_b is the Boltzmann constant and T_k is the absolute temperature) and relatively shallow secondary minimums (–6.8 K_bT_K at 50 mM to –1.1 K_bT_K at 1 mM). However, some discrepancy was observed at the IS of 50 mM because there is no colloids detected in the effluent (C_i/C_0=0) during the first two phases when DLVO theory predicted the repulsive energy barrier of 29 K_bT_K. One plausible explanation is, in this case, the electrostatic double layer of the soil colloidal particles was considerably compressed, and relatively large amounts of Cu (divalent cation) strongly adsorbed on the surface of WDSC enhanced the aggregation of the soil colloidal particles in the presence of OM (especially humic acid) that occurs. That is, in the presence of organic matter coating of the soil colloidal particles, the organic matter macromolecules aggregated through intermolecular bridging via Cu complexation to form organic matter aggregates, resulting in great deposition. Similar phenomenon was reported by Chen and Elimelech (2007).

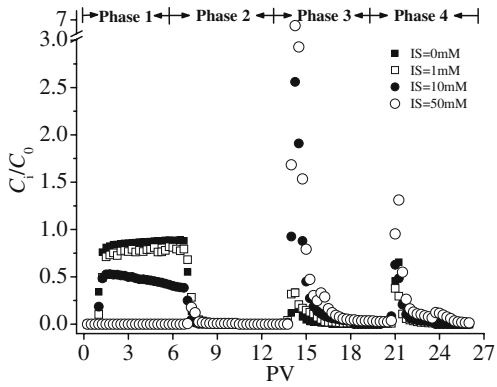

Fig. 5 Representative breakthrough curves for soil colloid at different ISs. Phase 1: 0–6 PVs, colloidal particles suspended in different ISs; phase 2: 6–13 PVs, colloid-free background electrolyte solution; phase 3: 13–20 PVs, change to ultrapure water (IS=0); phase 4: 20–26 PVs, colloid-free NaOH solution at pH 11

Figure 4 also presents the recovered colloid concentrations in the effluent as a function of PVs after flushing the column with ultrapure water (IS=0) at phase 3. The observed peak upon change of solution IS has typically been ascribed to the release of colloids that were deposited in the secondary minimum (Franchi and O'Melia 2003). In fact, the release of previously deposited colloidal particles through lowering bulk solution IS has been used as supportive evidence for particles deposited in the secondary minimum. Table 2 revealed the mass fraction of injected soil colloids that were recovered during elution with ultrapure water (MR_3). It showed that a large portion of the input colloids were recovered in the effluent and that MR_3 data range from 3.7% when the colloids were deposited with 1 mM solution to 68.5% when the colloids were deposited with 50 mM $NaNO_3$ solution. That MR_3 decreased with increasing IS of bulk solution because relatively less soil colloidal particles were retained in the secondary minimum at lower ISs (Table 4 and Fig. 6).

Mathematical expressions were used for a more quantitative characterization of the transport and deposition of soil colloids as revealed in Table 5. As observed, the soil colloids collision efficiency (α) is as a function of solution pH and IS. It is suggested that the results are qualitative in agreement with DLVO theory, that is, at higher ionic strength or lower solution pH, the diffuse layer is

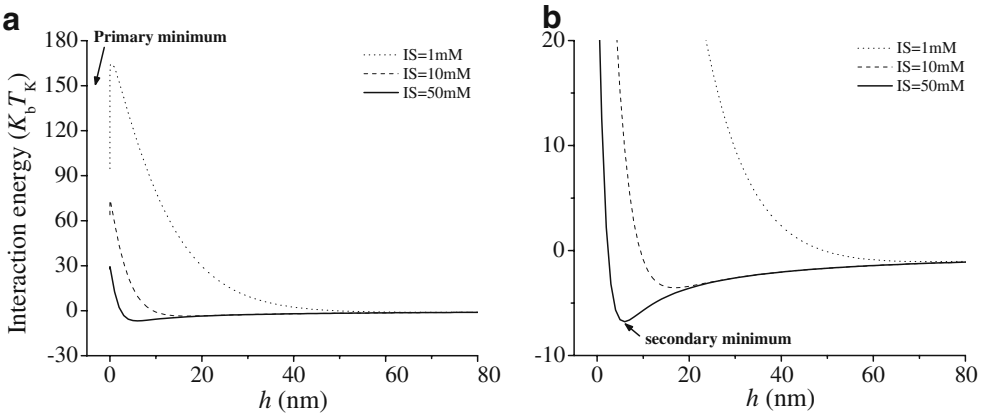

Fig. 6 Representative of the total interaction energy versus surface-to-surface separation distance profile for quartz sand and soil colloids under different ionic strength conditions. **a** The maximum repulsive energy barrier (Φ_{max}) that prevents attachment in the primary minimum. **b** The same data in enlarged beginning of the *y*-axis show the secondary minimum (Φ_{min2})

compressed causing a reduction in the repulsive electrostatic double layer forces and an increase in the soil colloids deposition. The change in solution composition from 0 to 10 mM $NaNO_3$ yielded an increase in α from 0.15 to 1.0, and the change in solution pH from 2.97 to 8.94 yielded a great decrease in α from 1.0 to 0.035. Almost no colloid was detected in the effluent at the IS of 50 mM or the pH of 2.97 for the collision efficiency was equal to 1.0. Interestingly, the collision efficiency calculated in our experiment was significantly greater than those reported by other researchers (Bradford et al. 2002; Shen et al. 2007) in the same model system (quartz sand as the collector grain). The collision efficiency increased gently from 0.0036 to 0.0063 as the diameter of model colloids increased from 0.45 to 1.0 μm at the IS of 1 mM as reported by Bradford et al. (2002) which is nearly two orders of magnitude smaller than our result (0.16 at the same IS, see Table 5). Several potential explanations on the specific physicochemical properties of the WDSC used in the experiment were attributed to the discrepancy. Firstly, the presence of Cu, Fe, and Al (hydro)oxides of the WDSC enhancing the degree of surface charge heterogeneity (Tufenkji and Elimelech 2005) and creating "favorable nanoscale patches" (Duffadar and Davis 2008) led to great deposition of the colloidal particles. In the second place, surface roughness (Kretzschmar et al. 1997) arose from the board size distributions and irregular shapes of the WDSC (see Fig. 1) was another explanation. In addition, such as straining (Bradford et al. 2002) of the soil colloidal particles and non-DLVO forces (e.g., Lewis acid–base interactions, and steric interactions; Simoni et al. 2000) were deserved to account for the observed deviation.

4.4 Effect of NaOH solution on the re-entrainment of retained colloids deposited in the primary minimum

Figure 3b and Fig. 5 present the typical behavior of retained colloids re-entrain after flushing colloid-free NaOH solution (pH=11) at different pH and ISs, respectively. As observed, sudden peaks of the effluent concentration were achieved, and the instantaneous maximum C_i/C_0 was up to 7.6 at the initial solution pH of 2.97 and 1.3 at the IS of 50 mM. Meanwhile, the trends of C_i/C_0 during flushing colloid-free NaOH solution under different pH and ISs were similar to that of those mobilized colloids re-entrained from the secondary minimum through flushing ultrapure water under different ISs. Colloid concentrations in the effluent sharply dropped after the front and experienced small tails.

The effect of NaOH solution at pH 11 on re-entrainment of retained colloids deposited in the primary minimum into pore water solution as defined as FRE_{NaOH} was revealed in Table 2. It is obvious that the value of FRE_{NaOH} decreased with increasing solution pH and increased with increasing IS of bulk solution. The change in solution pH from 2.97 to 8.94 yielded a decrease in FRE_{NaOH} from 86.7% to 35.8%, and the change in solution composition from 0 to 50 mM

Table 5 Physical and calculated parameters for packed-bed column experiments

Experiment	pH	IS (mM)	Column length (cm)	MR_{12} (%)[a]	η_0[b]	α[c]
1	2.97	0	20.0	0.7	3.4×10^{-3}	1.00
2	4.98	0	20.0	75.9	3.6×10^{-3}	0.32
3	7.00	0	20.0	80.4	3.3×10^{-3}	0.15
4	8.94	0	20.0	89.4	3.4×10^{-3}	0.04
5	5.00	0	20.2	84.4	3.4×10^{-3}	0.15
6	5.00	1	20.2	79.9	3.7×10^{-3}	0.16
7	5.00	10	20.2	48.8	3.5×10^{-3}	0.60
8	5.00	50	20.2	1.7	3.6×10^{-3}	1.00

[a] MR_{12}, fraction of mass recovery of injected colloids from phases 1 and 2

[b] The single collector removal efficiency (η_0)

[c] The collision efficiency (α) as revealed in Section 3

$NaNO_3$ yielded an increase in FRE_{NaOH} from 38.6% to 64.6%. In practice, when flushing NaOH solution, the surface charges of these retained colloidal particles were altered, thus enhancing their re-entrainment from the primary minimum well. Therefore, it is clear that NaOH solution at pH 11 poses a predominant role on mobilization of those colloids deposited in the primary minimum during the whole re-entrainment experiment.

The role of NaOH solution at high pH on re-entrainment of colloids deposited in the primary minimum was always ignored by most researchers who select model colloids because the influence of NaOH solution on the model colloids was little in saturated packed column; however, it was considerably necessary to investigate its effect on the transport and fate of natural soil colloids. Here, the effect was impressive in our experiment. Below, we will examine several potential explanations for the observed impressive effect. In the first place, in high concentration of NaOH solution, montmorillonite colloidal particles existed in WDSC can exchange with sodium in the bulk solution that promote the dispersion which involves the breakdown of large aggregates into individual particles. Meanwhile, the mobility of individual particles is relatively stronger than large aggregates resulting in a large portion of mobilization of those retained colloids. Secondly, the presence of kaolinite colloidal particles is another key factor. Associations between positive edges and negative surfaces cause internal mutual flocculation between kaolinite particles at pH 5 (the pH of pore water solution before flushing NaOH solution). Nevertheless, NaOH solution at pH 11 can lead to conversion of edge charge from positive to negative which increases the electrostatic repulsion interaction between edges and surfaces, and particles and particles (Churchman et al. 1993). In addition, the conversion of surface charge from positive to negative of the Fe and Al (hydro)oxides due to deprotonation of the surface sites and dissociation of organic matter coating (Schuwirth and Hofmann 2006) of the WDSC at pH 11 are also account for the effect. Thus, a large portion of the retained colloids were recovered from the primary minimum, and NaOH at pH 11 posed a predominant role on the mobilization of those retained colloids.

Table 2 also presents the mass recovery of the introduced soil colloids in the effluent during dissection experiment (MR_s). As observed, still a small amount of input colloids were recovered even after flushing NaOH solution. The MR_s decreased from 13.2% to 6.8% with increasing pH from 2.97 to 8.94 and increased from 7.3% to 10.7% with increasing IS from 0 to 50 mM. One potential explanation is ascribed that the aggregation of the deposited colloids may have occurred near grain–grain contracts, and the colloidal particles are prone to aggregate to form lager particles at lower pH or high IS conditions. Similar phenomenon that colloid aggregation occurred near grain–grain contacts that points under unfavorable conditions was observed by Li et al. (2006).

4.5 Cotransport behavior of soil colloids and colloid-facilitated Cu at different ISs

Figure 7 shows cotransport behavior of soil colloids and the Cu strongly adsorbed on the soil colloids at the IS of zero. As observed, the amount of dissolved Cu was very low (almost below the value of 5 μg L^{-1}), while colloid-facilitated Cu occupied relatively high values of about 85 μg L^{-1} when the effluent reached to a steady-state flow (the first two phases). Upon stepwise change in solution chemistry, soil colloids and colloid-facilitated Cu (colloid-F Cu) concurrently transported with pore water flow, and nearly no dissolved Cu was detected in the effluent. In practice, the Cu adsorbed on soil colloidal particles nearly cannot be detached from its carriers under the competition of coexisted cations (e.g., Na^+) in the bulk solution. It is therefore that no dissolved Cu was detected in the effluent during phases 3 and 4. Similar results were observed under other ISs (Fig. 8).

Our results demonstrate that the strongly adsorbed Cu on soil colloids almost cannot be detached from its carrier under the competition of cations existed of the bulk solution and will cotransport with its carrier under transient solution chemistry conditions in saturated columns packed with quartz sand. Similar results are reported by Badin et al. (2009) who concluded that the mobilities of heavy metals are highly correlated with their carriers in natural soil system. It is therefore that colloid-facilitated transport of strongly absorbing contaminant is assumed to be posed considerable contamination risks at distant locations from

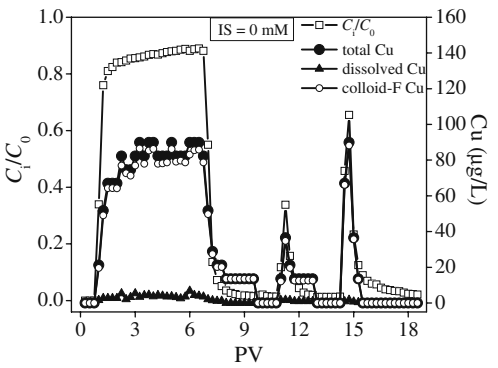

Fig. 7 Representative breakthrough curves of soil colloids, and dissolved Cu and colloid-facilitated Cu (*colloid-F Cu*), and total Cu as a function of PVs at the IS of 0. Phase 1: 0–6 PVs, colloidal particles suspended in different ISs; phase 2: 6–13 PVs, colloid-free background electrolyte solution; phase 3: 13–20 PVs, change to ultrapure water (IS=0); phase 4: 20–26 PVs, colloid-free NaOH solution at pH 11

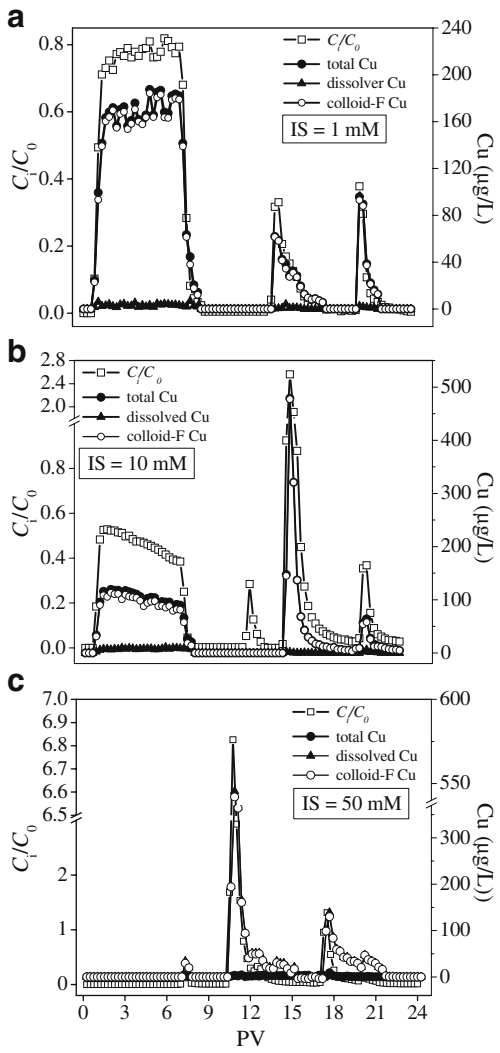

Fig. 8 Representative breakthrough curves of soil colloids, and dissolved Cu and colloid-facilitated Cu (*colloid-F Cu*), and total Cu as a function of PVs at different ISs. Note that **a**, **b**, and **c** represent IS of the bulk solution of 1, 10, and 50 mM, respectively. Phase 1: 0–6 PVs, colloidal particles suspended in different ISs; phase 2: 6–13 PVs, colloid-free background electrolyte solution; phase 3: 13–20 PVs, change to ultrapure water (IS=0); phase 4: 20–26 PVs, colloid-free NaOH solution at pH 11

the pollutant source if the IS of pore water that was low or its pH was high, or both. Meanwhile, it can be inferred that chemical transients, produced by the introduction of low IS (e.g., rainfall, and snowmelt) and/or high pH NaOH solution into soil pore water, result in destabilization of colloidal aggregates in soils and mobilization of colloids and the contaminants adsorbed on them.

As to natural subsurface environments, transport and fate of WDSC and contaminants adsorbed on the WDSC are quite different because soils and sediments exhibit large variability in the roughness of mineral particles, composition, and relative proportions of minerals. In addition, sorbed ions, organic coating, and mineral precipitates on soil surfaces may also change the transport behaviors of the WDSC.

5 Conclusions

In this study, saturated columns packed with pure quartz sand were conducted to explore the mechanism of transport and re-entrainment of WDSC and facilitating the transport of Cu under different pH and ISs. It is suggested that the colloid collision efficiency decreased as the pH of bulk solution increased and the ionic strength of bulk solution decreased, and NaOH solution at pH 11 poses a predominant role on the mobilization of retained colloids deposited in the primary minimum. Meanwhile, the Cu strongly adsorbed on soil colloids nearly cannot be detached from its carrier under the competition of coexisted cations in the bulk solution and cotransport with its carrier under different ionic strengths in saturated systems.

6 Recommendations and perspectives

Natural organic matter (NOM), omnipresent in aquatic environments and soils, is one of the key factors governing the environmental transport and fate of soil colloids. NOM can adsorb onto soil colloidal particles, increase their surface negative charges, and consequently promote their transport behaviors.

Goethite is a primary type of iron oxide in soils and on suspended particles in natural water bodies (Sposito 2008). It has been widely used as a representative of iron oxides coating on aquifer sediments to characterize the mechanisms of surface reaction in numerous studies. The presence of goethite coating on aquifer sediments at circumneutral pH can result in positively charged sediment surfaces which readily adsorb soil colloidal particles at the pH conditions and consequently inhibit their transport behaviors.

Mobile soil colloids are omnipresent in the pore water of the subsurface systems such as soils, groundwater aquifer, sediments, and fractured rocks. Considering the antagonistic effects of NOM and goethite coating on the transport behavior of soil colloids, it is considerably urgent to explore the mechanism of transport and fate of soil colloids on the effect of NOM, goethite-coating, or both in saturated packed columns.

Acknowledgments We thank the support of the Knowledge Innovative project of Chinese Academy of Sciences (KZCX2-YW-Q02-02) and the open fund of the State Key Laboratory of Soil and Sustainable Agriculture (Y052010027). We also thank Dr. Jun Jiang (Institute of Soil Science, Chinese Academy of Sciences) for helping the measurement of the ζ-potentials of soil colloids.

References

Badin AL, Bedell JP, Delolme C (2009) Effect of water content on aggregation and contaminant leaching: the study of an urban Technosol. J Soils Sediments 9:653–663

Baveye P, Vandevivere P, Hoyle BL, DeLeo PC, de Lozada DS (1998) Environmental impact and mechanisms of the biological clogging of saturated soils and aquifer materials. Crit Rev Env Sci Tec 28:123–191

Bradford SA, Yates SR, Bettahar M, Simunek J (2002) Physical factors affecting the transport and fate of colloids in saturated porous media. Water Resour Res 38(12):1327. doi:10.1029/2002WR001340

Bradl HB (2004) Adsorption of heavy metal ions on soils and soils constituents. J Colloid Interf Sci 277:1–18

Chen KL, Elimelech M (2007) Influence of humic acid on the aggregation kinetics of fullerene (C-60) nanoparticles in monovalent and divalent electrolyte solutions. J Colloid Interf Sci 309:126–134

Churchman GJ, Skjemstad JO, Oades JM (1993) Influence of clay-minerals and organic-matter on effects of sodicity on soils. Aust J Soil Res 31:779–800

DeNovio NM, Saiers JE, Ryan JN (2004) Colloid movement in unsaturated porous media: recent advances and future directions. Vadose Zone J 3:338–351

Derjaguin B, Landau L (1993) Theory of the stability of strongly charged lyophobic sols and of the adhesion of strongly charged-particles in solutions of electrolytes. Prog Surf Sci 43:30–59

Duffadar RD, Davis JM (2008) Dynamic adhesion behavior of micrometer-scale particles flowing over patchy surfaces with nano-scale electrostatic heterogeneity. J Colloid Interf Sci 326:18–27

Elimelech M, Omelia CR (1990) Kinetics of deposition of colloidal particles in porous-media. Environ Sci Technol 24:1528–1536

Elimelech M, Gregory J, Jia X, Williams RA (1995) Particle deposition and aggregation: measurement, modeling and simulation. Butterworth-Heinemann, Oxford

Elimelech M, Nagai M, Ko CH, Ryan JN (2000) Relative insignificance of mineral grain zeta potential to colloid transport in geochemically heterogeneous porous media. Environ Sci Technol 34:2143–2148

Ferreira TO, Otero XL, de Souza VS, Vidal-Torrado P, Macias F, Firme LP (2010) Spatial patterns of soil attributes and components in a mangrove system in Southeast Brazil (So Paulo). J Soils Sediments 10:995–1006

Franchi A, O'Melia CR (2003) Effects of natural organic matter and solution chemistry on the deposition and reentrainment of colloids in porous media. Environ Sci Technol 37:1122–1129

Gerbersdorf SU, Jancke T, Westrich B (2007) Sediment properties for assessing the erosion risk of contaminated riverine sites. J Soils Sediments 7:25–35

Goldberg S, Forster HS (1990) Flocculation of reference clays and arid-zone soil clays. Soil Sci Soc Am J 54:714–718

Grafe M, Eick MJ, Grossl PR (2001) Adsorption of arsenate (V) and arsenite (III) on goethite in the presence and absence of dissolved organic carbon. Soil Sci Soc Am J 65:1680–1687

Gregory J (1981) Approximate expressions for retarded van der Waals interaction. J Colloid Interf Sci 83:138–145

Grolimund D, Elimelech M, Borkovec M, Barmettler K, Kretzschmar R, Sticher H (1998) Transport of in situ mobilized colloidal particles in packed soil columns. Environ Sci Technol 32:3562–3569

Harvey RW, Garabedian SP (1991) Use of colloid filtration theory in modeling movement of bacteria through a contaminated sandy aquifer. Environ Sci Technol 25:178–185

Hogg R, Healy TW, Fuersten Dw (1966) Mutual coagulation of colloidal dispersions. T Faraday Soc 62:1638

Hunter RJ (1981) Zeta potential in colloid science: principles and applications. Academic, New York

Hunter RJ (1986) Foundations of colloid science. Oxford University Press, Oxford

Jaisi DP, Elimelech M (2009) Single-walled carbon nanotubes exhibit limited transport in soil columns. Environ Sci Technol 43:9161–9166

Karathanasis AD (1999) Subsurface migration of copper and zinc mediated by soil colloids. Soil Sci Soc Am J 63:830–838

Kersting AB, Efurd DW, Finnegan DL, Rokop DJ, Smith DK, Thompson JL (1999) Migration of plutonium in ground water at the Nevada Test Site. Nature 397:56–59

Khilar KC, Fogler HS (1984) The Existence of a critical salt concentration for particle release. J Colloid Interf Sci 101:214–224

Kretzschmar R, Barmettler K, Grolimund D, Yan YD, Borkovec M, Sticher H (1997) Experimental determination of colloid deposition rates and collision efficiencies in natural porous media. Water Resour Res 33:1129–1137

Kretzschmar R, Holthoff H, Sticher H (1998) Influence of pH and humic acid on coagulation kinetics of kaolinite: a dynamic light scattering study. J Colloid Interf Sci 202:95–103

Lenhart JJ, Saiers JE (2003) Colloid mobilization in water-saturated porous media under transient chemical conditions. Environ Sci Technol 37:2780–2787

Li XQ, Lin CL, Miller JD, Johnson WP (2006) Role of grain-to-grain contacts on profiles of retained colloids in porous media in the presence of an energy barrier to deposition. Environ Sci Technol 40:3769–3774

McCarthy JF, McKay LD (2004) Colloid transport in the subsurface: past, present, and future challenges. Vadose Zone J 3:326–337

Posadas AND, Gimenez D, Bittelli M, Vaz CMP, Flury M (2001) Multifractal characterization of soil particle-size distributions. Soil Sci Soc Am J 65:1361–1367

Ryan JN, Elimelech M (1996) Colloid mobilization and transport in groundwater. Colloid Surf A 107:1–56

Schuwirth N, Hofmann T (2006) Comparability of and alternatives to leaching tests for the assessment of the emission of inorganic soil contamination. J Soils Sediments 6:102–112

Sen TK, Mahajan SP, Khilar KC (2002) Colloid-associated contaminant transport in porous media: 1. Experimental studies. Aiche J 48:2366–2374

Shen CY, Li BG, Huang YF, Jin Y (2007) Kinetics of coupled primary- and secondary-minimum deposition of colloids under unfavorable chemical conditions. Environ Sci Technol 41:6976–6982

Simoni SF, Bosma TNP, Harms H, Zehnder AJB (2000) Bivalent cations increase both the subpopulation of adhering bacteria and their adhesion efficiency in sand columns. Environ Sci Technol 34:1011–1017

Sposito G (2008) The chemistry of soils. Oxford University Press, USA

Torkzaban S, Tazehkand SS, Walker SL, Bradford SA (2008) Transport and fate of bacteria in porous media: coupled effects of chemical conditions and pore space geometry. Water Resour Res 44:W04403. doi:10.1029/2007WR006541

Tosco T, Tiraferri A, Sethi R (2009) Ionic strength dependent transport of microparticles in saturated porous media: modeling mobilization and immobilization phenomena under transient chemical conditions. Environ Sci Technol 43:4425–4431

Tufenkji N, Elimelech M (2004) Correlation equation for predicting single-collector efficiency in physicochemical filtration in saturated porous media. Environ Sci Technol 38:529–536

Tufenkji N, Elimelech M (2005) Breakdown of colloid filtration theory: role of the secondary energy minimum and surface charge heterogeneities. Langmuir 21:841–852

Usman A, Kuzyakov Y, Stahr K (2005) Effect of clay minerals on immobilization of heavy metals and microbial activity in a

sewage sludge-contaminated soil. J Soils Sediments 5:245–252

Verwey EJW, Overbeek JTG (1948) Theory of the stability of lyophobic colloids. Elsevier, Amsterdam

Wan JM, Tokunaga TK (2002) Partitioning of clay colloids at air-water interfaces. J Colloid Interf Sci 247:54–61

Wilkinson KJ, Balnois E, Leppard GG, Buffle J (1999) Characteristic features of the major components of freshwater colloidal organic matter revealed by transmission electron and atomic force microscopy. Colloid Surf A 155:287–310

Xiong Y (1985) Soil colloids: the investigation method on soil colloids (in Chinese). Science Press, Beijing, pp 8–14